



Article

# BrCWM Mutation Disrupted Leaf Flattening in Chinese Cabbage (*Brassica rapa* L. ssp. *pekinensis*)

Yanji Wu, Yue Xin, Jiaqi Zou, Shengnan Huang, Che Wang and Hui Feng \*

Liaoning Key Laboratory of Genetics and Breeding for Cruciferous Vegetable Crops, College of Horticulture, Shenyang Agricultural University, Shenyang 110065, China

\* Correspondence: fenghuiaaa@syau.edu.cn; Tel.: +86-1389-889-9863

**Abstract:** Leaf flattening plays a vital role in the establishment of plant architecture, which is closely related to plant photosynthesis and, thus, influences the product yield and quality of Chinese cabbage. In this study, we used the doubled haploid line ‘FT’ of Chinese cabbage as the wild type for ethyl methanesulfonate (EMS) mutagenesis and obtained a mutant *cwm* with stably inherited compact and wrinkled leaves. Genetic analysis revealed that the mutated trait was controlled by a single recessive nuclear gene, *Brcwm*. *Brcwm* was preliminarily mapped to chromosome A07 based on bulked segregant RNA sequencing (BSR-seq) and fine-mapped to a 205.66 kb region containing 39 genes between Indel12 and Indel21 using SSR and Indel analysis. According to the whole-genome re-sequencing results, we found that there was only one nonsynonymous single nucleotide polymorphism (SNP) (C to T) within the target interval on exon 4 of *BraA07g021970.3C*, which resulted in a proline to serine amino acid substitution. The mutated trait co-segregated with the SNP. Quantitative reverse transcriptase polymerase chain reaction (qRT-PCR) revealed that *BraA07g021970.3C* expression was dramatically higher in ‘FT’ leaves than that in *cwm* leaves. *BraA07g021970.3C* is homologous to *AT3G55000* encoding a protein related to cortical microtubule organization. A similar phenotype of dwarfism and wrinkled leaves was observed in the recessive homozygous mutant *cwm-f1* of *AT3G55000*, and its T3 transgenic lines were restored to the *Arabidopsis* wild-type phenotype through ectopic overexpression of *BraA07g021970.3C*. These results verified that *BraA07g021970.3C* was the target gene essential for leaf flattening in Chinese cabbage.

**Keywords:** Chinese cabbage; wrinkled leaves; cortical microtubule; gene cloning; mutant



**Citation:** Wu, Y.; Xin, Y.; Zou, J.; Huang, S.; Wang, C.; Feng, H. BrCWM Mutation Disrupted Leaf Flattening in Chinese Cabbage (*Brassica rapa* L. ssp. *pekinensis*). *Int. J. Mol. Sci.* **2023**, *24*, 5225. <https://doi.org/10.3390/ijms24065225>

Academic Editor: Maoteng Li

Received: 8 February 2023

Revised: 4 March 2023

Accepted: 7 March 2023

Published: 9 March 2023



**Copyright:** © 2023 by the authors. Licensee MDPI, Basel, Switzerland. This article is an open access article distributed under the terms and conditions of the Creative Commons Attribution (CC BY) license (<https://creativecommons.org/licenses/by/4.0/>).

## 1. Introduction

Leaves are the most important photosynthetic organs in plants, and their morphology and functionality directly determine crop productivity by affecting plant architecture, respiration, transpiration, and nutrient absorption [1,2]. For most plants, their leaves would develop into flat laminas, which is a natural adaptation to enlarge the area for capturing light. Therefore, leaf flattening is an important agronomic trait for crop breeding.

Leaf morphological development is a complicated process regulated by transcription factors, gene expression, and environmental factors [3]. Several mutants related to leaf flatness have been identified and their mutant genes have been mapped and cloned. NJAU5737, with up curled and slightly crinkled leaves, has been identified in *Brassica napus*. On chromosome A05, an 83.19 kb interval contained the dominant locus (*BnUC2*) that controls the trait. The candidate gene *BnaA05g16700D* encodes a regulatory protein for auxin signal transcription [4]. Two curly leaf mutants, *cul-1* and *cul-2* have been identified in cucumber. The mutant gene is mapped to chromosome 6 in a 128 kb region. As the candidate gene, *CsPHB* encodes the HD-ZIP III transcription factor [5]. Research has shown that in the RL-D mutant, a single dominant gene controls the leaf-rolling trait and is located on rice chromosome 3 within a 743 kb region. The candidate gene identified is *Os03g0395100*, which encodes a protein phosphatase [6]. *lad1* is a rolling-leaf mutant of

rice. The mutant gene *KAN1* maps on chromosome 9 within 34 kb intervals. The candidate gene *KAN1* interacts with ARF3, ARF7, and ARF15, playing a conservative role during leaf development [7]. These studies provide valuable genetic resources and references for elucidating the mechanisms underlying leaf morphology and plant development.

Plant microtubules (MTs) are subcellular nanotubes composed of  $\alpha$ -tubulin and  $\beta$ -tubulin that participate in cell mitosis, intracellular material transport, cell wall construction, morphogenesis, and polarity establishment [8–12]. During the cell cycle, MTs are present in four distinct arrays: cortical microtubules (CMTs), preprophase band (PPB), spindle, and phragmoplast. In response to microtubule arrays, microtubule-associated proteins (MAPs) bind to microtubules and modulate their functions. Recent studies have shown that MAPs, such as MOR1, TRM, FASS, TON1, kinesins, CLASP, and TAN1, affect microtubule arrays and plant development [13–17]. Among these genes, TON1 has been reported to be a cortical microtubule-related protein. Studies have shown that the disruption of *TON1* leads to the disappearance of PPB, and the *TON1* deletion mutant displays irregular cell elongation and division planes [15,16]. As a matter of fact, the role of TON1 homologous proteins in the plant development of horticultural crops remains largely unknown.

Chinese cabbage is widely cultivated in Eastern Asia. As a vital vegetable crop, its leaves are not only the photosynthetic apparatus but also the main product organ. Leaf morphology directly affects yield and commodity value. In this study, a compact and wrinkled mutant *cwm* was obtained from an ethyl methanesulfonate (EMS) mutagenesis population of Chinese cabbage, and the molecular mechanism of leaf flattening was explored. *BraA07g021970.3C* was referred to as the candidate gene for mutation traits using bulked segregant RNA sequencing (BSR-seq) and whole-genome re-sequencing. The *Arabidopsis cwm-f1* mutant with wrinkled leaves restored its normal phenotype by ectopic overexpression of *BrCWM*.

## 2. Results

### 2.1. Morphological Characterization of the Mutant *Cwm*

*cwm* exhibited a compact plant with wrinkled leaves in contrast to the wild type 'FT' (Figure 1A). The mutant leafy head was remarkably smaller than 'FT' (Figure 1B; Table S5). Based on the growth curves, leaf length, leaf width, and plant width increased more slowly in *cwm* following the appearance of the third true leaf (Figure 1C).

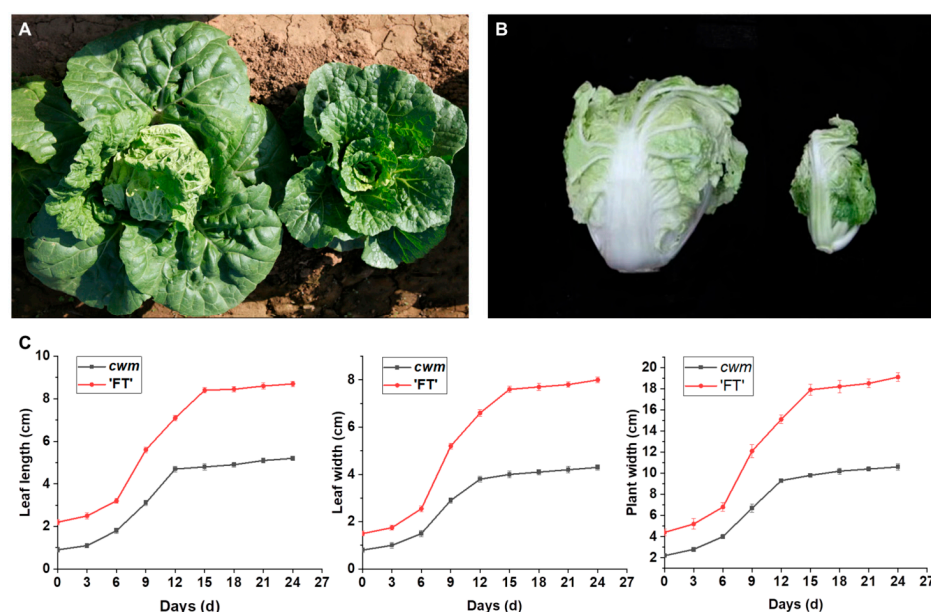


**Figure 1.** Phenotypic characterization of 'FT' and *cwm*. (A) The phenotypic characterization of 'FT' (left) and *cwm* (right) at the heading stage. (B) The identification of leafy heads in 'FT' (left) and *cwm* (right). (C) The growth curves of *cwm* and 'FT' at the seedling stage.

To further characterize the leaf morphology, the paraffin sections were performed. In *cwm*, there were more vascular bundles and thicker leaves, and in both spongy mesophyll and palisade mesophyll, the lacunas were larger, compared to 'FT'. (Figure 2).

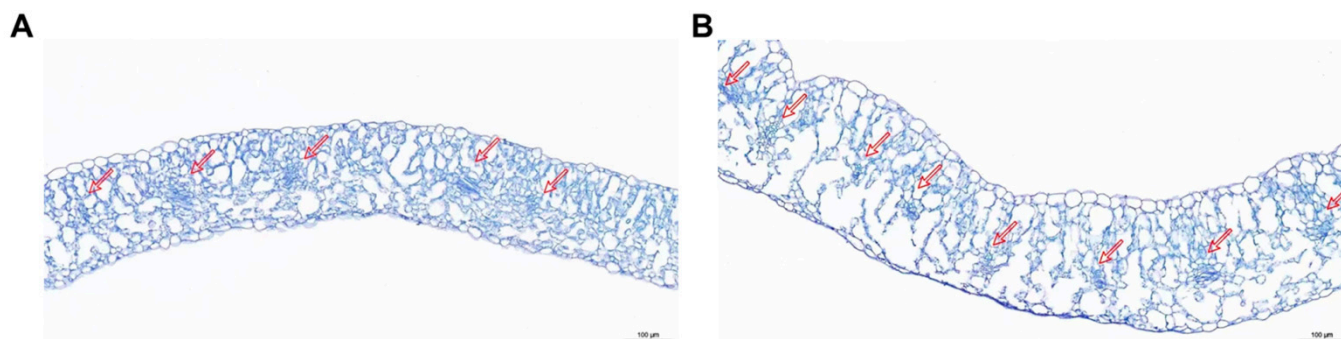


**Figure 2.** Paraffin section of the leaf transverse section. Scale bar = 100  $\mu\text{m}$ . (A) Leaf transverse sections of 'FT'. (B) Leaf transverse sections of *cwm*. The red arrows indicated the vascular bundles in the leaf mesophyll.

### 2.2. Inheritance of the Mutated Traits

The results of the genetic analysis are listed in Table 1. All  $F_1$  plants exhibited the wild-type phenotype, indicating that the mutant traits were controlled by a recessive gene. Among the 250  $F_2$  individuals, 184 plants exhibited wild-type traits, while the rest exhibited mutant traits, in consonance with the segregation ratio of 3:1 ( $\chi^2 = 0.192$ ). Forty plants from  $BC_1$  ( $F_1 \times \text{'FT'}$ ) were all same as the 'FT' phenotype. Among the  $BC_1$  ( $F_1 \times cwm$ ) plants, 19 and 21 showed the 'FT' phenotype and *cwm* phenotype, respectively, which conformed to a segregation ratio of 1:1 ( $\chi^2 = 0.100$ ). Taken together, these mutant traits were controlled by a single recessive nuclear gene, *Brcwm*.

**Table 1.** Genetic analysis of the wrinkled leaves phenotype in mutant *cwm*.

| Generation                    | Normal Leaves | Wrinkled Leaves | Segregation Ratio | Expected Ratio | $\chi^2$ |
|-------------------------------|---------------|-----------------|-------------------|----------------|----------|
| $P_1$ (FT)                    | 50            | 0               |                   |                |          |
| $P_2$ ( <i>cwm</i> )          | 0             | 50              |                   |                |          |
| $P_1 \times P_2$              | 35            | 0               |                   |                |          |
| $P_2 \times P_1$              | 35            | 0               |                   |                |          |
| $(P_1 \times P_2) \times P_1$ | 40            | 0               |                   |                |          |
| $(P_1 \times P_2) \times P_2$ | 19            | 21              | 1.167:1           | 1:1            | 0.100    |
| $F_2$                         | 184           | 66              | 2.787:1           | 3:1            | 0.192    |

### 2.3. Preliminary Mapping of *Brcwm* Using BSR-Seq

*Brcwm* was preliminarily mapped using BSR-Seq. Among the 39,346,988 and 41,518,202 clean reads within the mutation pool and wild-type pool, respectively, the GC content and Q30 (the base quality value was 30, and the error rate was 0.1%) percentage revealed that the sequencing data were extremely precise (Table 2). The total mapping ratio from clean reads to Brara\_Chiifu\_V3.0 (<http://brassicadb.cn>, accessed on 5 May 2022) was  $0.81 > 0.7$ , suggesting that there were high sequence similarities between them (Table 2). Using the analysis of the single-nucleotide variant (SNV) difference and the value of Euclidean distance<sup>5</sup> ( $ED^5$ ), the distribution of  $ED^5$  values on the chromosomes was illustrated (Figure 3). The *Brcwm* loci were located in four target candidate regions: A05 24538973-26614010, A07 10076460-11983310, A07 13806342-15548454, and A07 17469944-20228803 (Table 3).

**Table 2.** Summary of clean Illumina RNA-Seq reads from ‘FT’ and *cwm* samples.

| Sample     | Total Raw Reads | Total Clean Reads | Total Mapping | Total Mapping Ratio | Q30 (%) | GC Content (%) |
|------------|-----------------|-------------------|---------------|---------------------|---------|----------------|
| ‘FT’       | 39,548,850      | 39,346,988        | 31,994,128    | 0.81                | 95.23   | 48.22          |
| <i>cwm</i> | 41,723,712      | 41,518,202        | 33,960,896    | 0.81                | 95.23   | 48.30          |

**Figure 3.** Map of ED<sup>5</sup> distribution on chromosomes. The width of each color on the X-axis represented the quantity of different SNV sites on each chromosome. The Y-axis represented the ED<sup>5</sup> values of each differential SNV site. The horizontal line referred to the threshold of the top 1%.**Table 3.** Localization of chromosome regions associated with the mutant traits.

| Chromosome | Start Site | End Site   | SNV Count | Target Length |
|------------|------------|------------|-----------|---------------|
| A05        | 24,538,973 | 26,614,010 | 25        | 2,075,037     |
| A07        | 10,076,460 | 11,983,310 | 20        | 1,906,850     |
| A07        | 13,806,342 | 15,548,454 | 28        | 1,742,112     |
| A07        | 17,469,944 | 20,228,803 | 57        | 2,758,859     |

To further narrow the range of *Brcwm* locations, a total of 15 pairs of polymorphic primers were screened out from 98 designed SSR primers. Three hundred recessive homozygous F<sub>2</sub> individuals were used to validate that SSR2227 and SSR3232 on A07 were closely linked to *Brcwm* (Figure S1, Table S1). Thus, *Brcwm* was mapped on chromosome A07 between markers SSR2227 and SSR3232, with 1.23 cM and 1.11 cM genetic distances, respectively (Figure 4A).

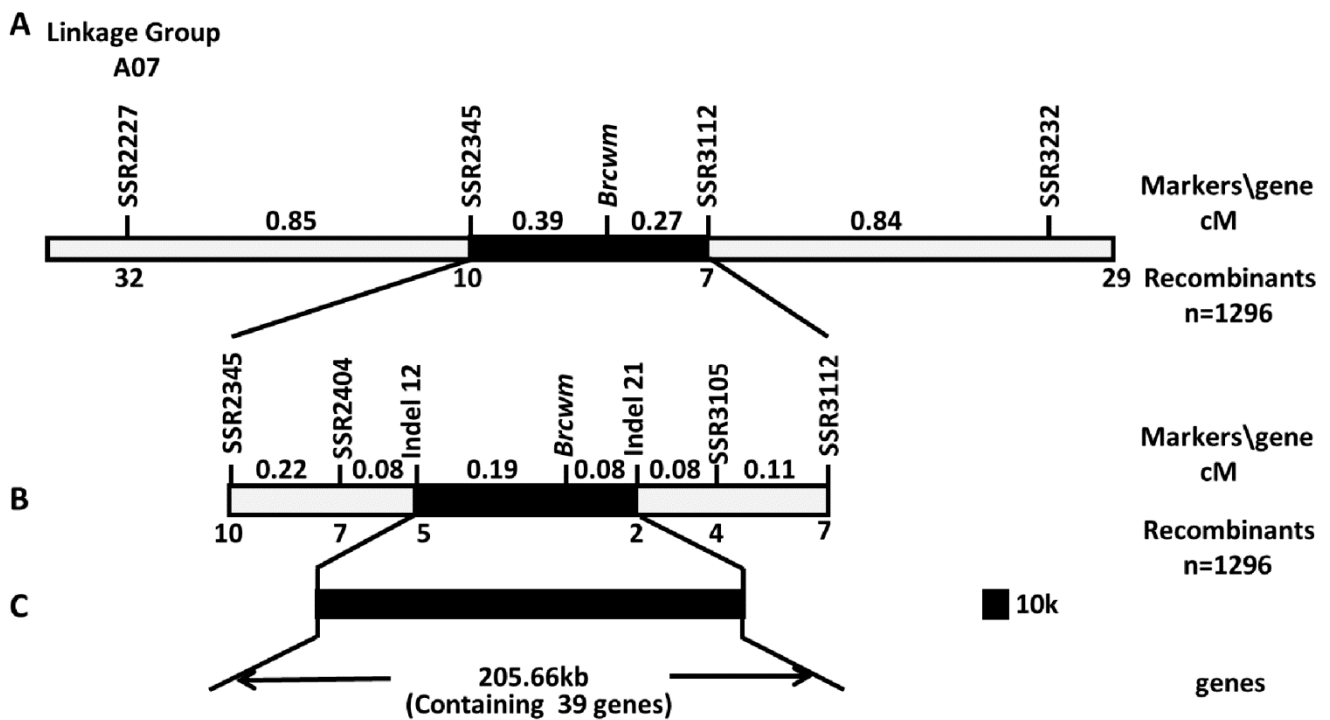


**Figure 4.** Mapping of the candidate gene. (A) Preliminary mapping of *Brcwm* based on the SSR primers screening recombinants. (B) Fine mapping of *Brcwm* based on the SSR and InDel primers screening recombinants. (C) Candidate gene analysis of *Brcwm*. In total, 1296  $F_2$  recessive individuals with wrinkled leaves phenotype were screened to construct the linkage map of chromosome A07. The figures (cM) above chromosome A07 stood for the genetic distance. The figures under chromosome A07 stood for the recombinants.

#### 2.4. Fine Mapping of *Brcwm*

To identify the mutation loci, 70 newly designed SSR and InDel markers were developed between markers SSR2227 and SSR3232. SSR2345, SSR2404, Indel12, Indel21, SSR3105, and SSR3112 with polymorphic markers were screened. Based on the mapping population of 1296  $F_2$  plants with the mutant phenotype, *Brcwm* was mapped between Indel12 and Indel21 according to the label of recombinants, and the physical distance was about 205.66 kb (Figure 4B,C).

#### 2.5. Candidate Gene Screening for *Cwm* using Whole Genome Re-Sequencing

Within the candidate interval, there were 39 genes referring to the *Brassica* database (<http://brassicadb.cn/>, accessed on 5 May 2022) (Figure 4C). Whole-genome re-sequencing of the mapping parents was conducted, and there was only one nonsynonymous SNP(C-T) on the exons within the mapping region. Because the SNP was on the fourth exon of *BraA07g021970.3C*, we identified *BraA07g021970.3C* as the candidate gene for *Brcwm*. According to genome annotations, *BrCWM* is homologous to *AT3G55000*, which encodes a protein related to cortical microtubule organization.

#### 2.6. Clone Sequencing and Co-Segregation Analysis

Cloning and sequencing were conducted to confirm the variation in gene sequence between 'FT' and *cwm*. The results showed that a C to T substitution occurred in *cwm*, resulting in an amino acid change from Pro to Ser (Figures 5A,B and S2).

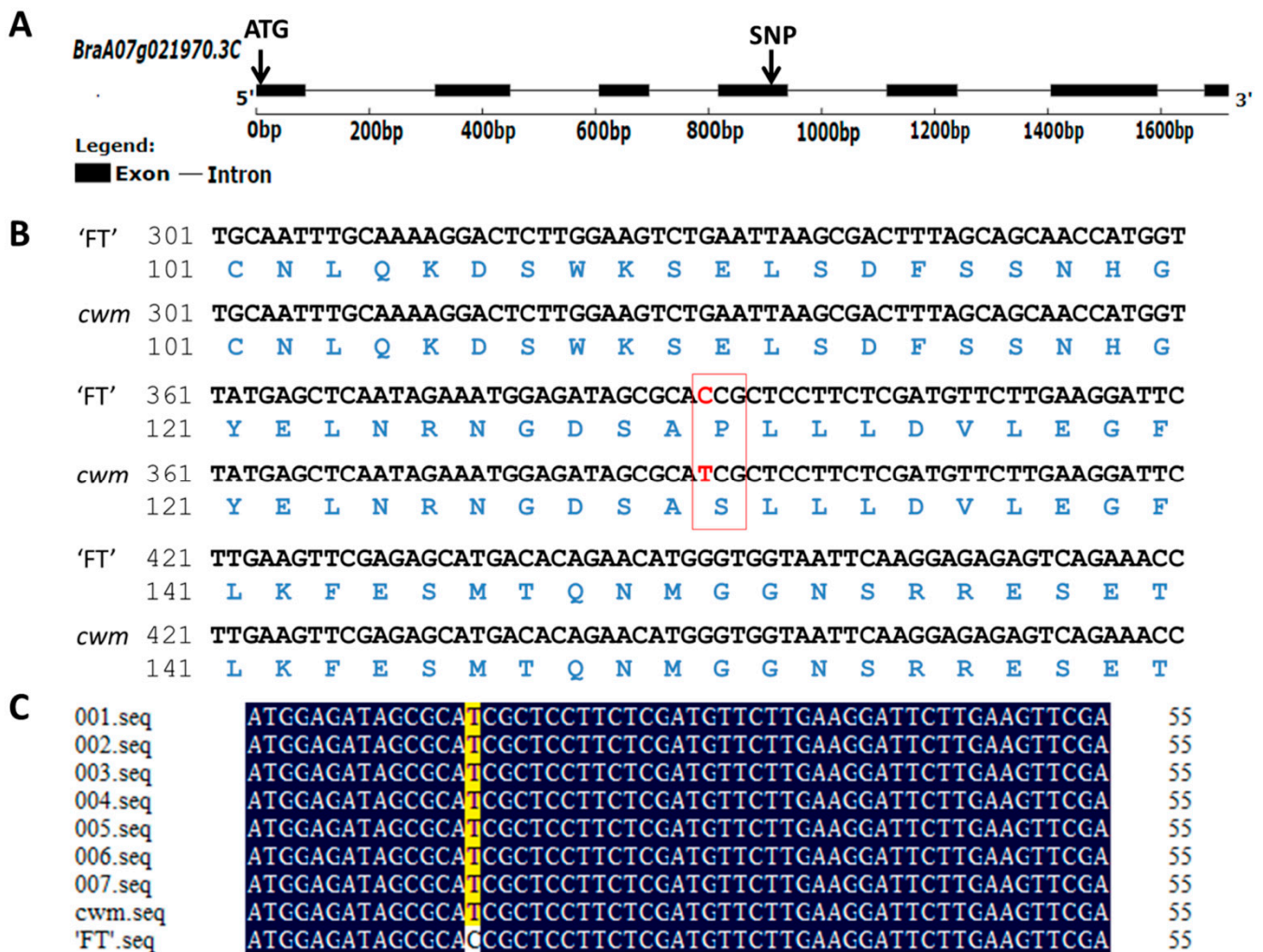


**Figure 5.** Gene structure, the alignment of gene sequence and amino acid sequence, and the co-segregation analysis. (A) Structure of *BraA07g021970.3C* with exon (the black square), intron (the black solid line), and nonsynonymous SNP and initiator codons (ATG). (B) Sequence alignments of partial amino acid and nucleotide of *BraA07g021970.3C* in 'FT' and *cwm*. The codons and amino acids in the red box resulted in the mutation. The nonsynonymous SNPs were shown in red color. (C) Sequence alignments of the *BraA07g021970.3C* nucleotides in seven  $F_2$  recombinants, *cwm*, and 'FT'. The seven  $F_2$  recombinants were screened by markers indel12 and indel21.

The mutation sites in seven recombinants identified by Indel12 and Indel21 were cloned, which were the same as those in *cwm*, indicating that this SNP co-segregated with the leaf wrinkled phenotype (Figure 5C). Thus, *BraA07g021970.3C* was confirmed as the causal gene for *cwm*.

### 2.7. Expression Analysis of BrCWM

To confirm whether there was a difference in *BraA07g021970.3C* expression levels between the wild-type and mutant, qRT-PCR was performed. The data demonstrated that whether in the leaves or roots, *BraA07g021970.3C* expressions were remarkably lower in *cwm* than that in 'FT' (Figure 6).

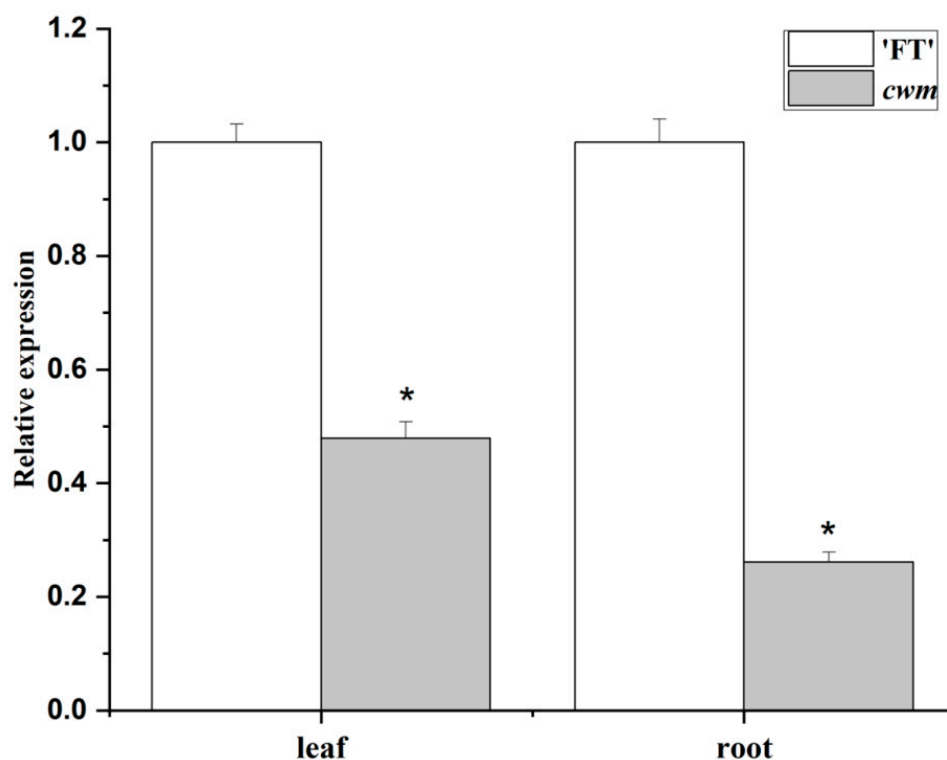


**Figure 6.** Expression levels of *BraA07g021970.3C* in leaves and roots were detected using qRT-PCR. Asterisks indicated statistical significance (Student's *t*-test, \*  $p < 0.05$ ).

### 2.8. Bioinformatic Analysis of BrCWM

To further elucidate the potential function of BrCWM, a series of bioinformatic analyses were performed. The result of TMHMM-2.0 forecasted that BrCWM has no transmembrane domain and is most likely a globular protein (Figure S3). The SWISS-MODEL software predicted that the substitution of amino acid residues in the mutation site resulted in tertiary structural changes in BrCWM, but there was no alteration in the holistic spatial structure (Figure 7). To clarify the possible phylogenetic relationship between BrCWM and other species, a phylogenetic tree was constructed using MEGA7 and NCBI BLAST. Eleven homologous proteins of BrCWM have been selected from other species. The results showed that the homology between BrCWM and *Raphanus sativus* TONNEAU 1a-like protein was the highest, reaching 92.37% (Figure 8).

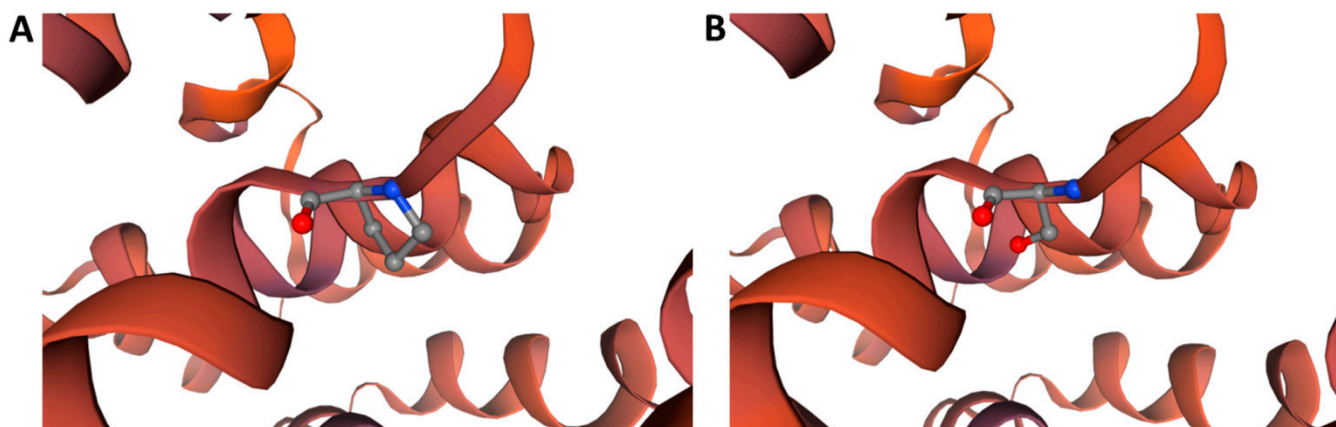


**Figure 7.** Protein tertiary structure analysis. (A) Tertiary structure of BrCWM. (B) Tertiary structure of the mutated BrCWM.

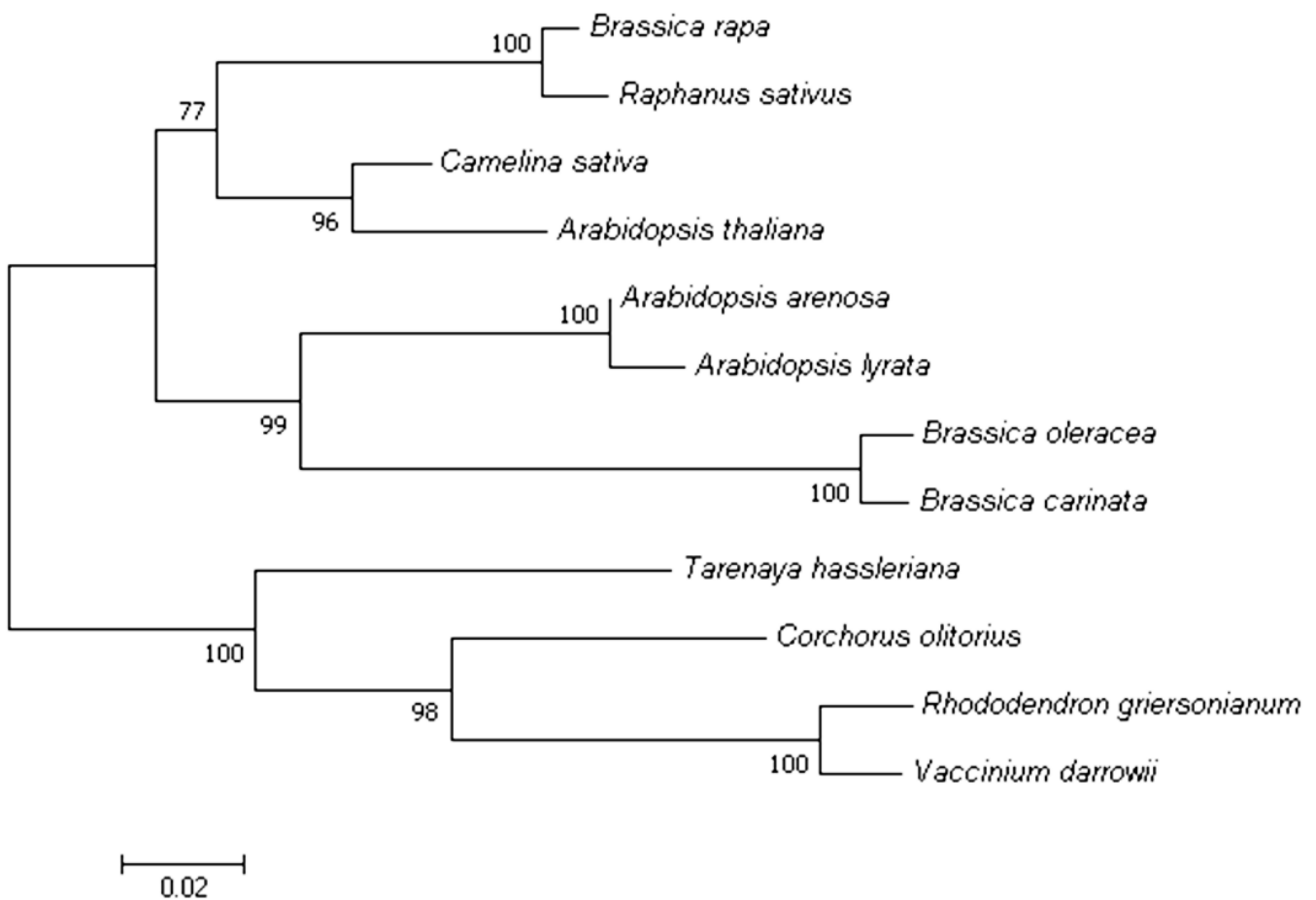


**Figure 8.** Phylogenetic tree analysis of BrCWM. The branch length which indicated evolutionary distance was drawn to scale.

### 2.9. Transgenic Functional Verification of BrCWM

BrCWM is homologous to AT3G55000. Mutation of AT3G55000 in *Arabidopsis ton1* resulted in the dysfunction of the cortical cytoskeleton and the absence of the preprophase band of microtubules, and the mutant plants were malformed [18]. In this study, we introduced *Arabidopsis cwm-f1* (CS2017348), an EMS-induced mutant that lacks the function of AT3G55000. The *cwm-f1* mutant exhibited wrinkled leaves and a dwarfing phenotype (Figure 9C). To verify whether BrCWM shares a similar function with *Arabidopsis AT3G55000*, we implemented an ectopic overexpression assay for *cwm-f1* by introducing 35S: BrCWM: GFP. Transgenic lines (homozygous T3-positive lines) were identified with PCR using primer W-1 (Figure 9A; Table S6). Col-0 and transgenic plants (BrCWM OX/*cwm-f1*) exhibited no significant morphological differences, whereas the leaf width of *cwm-f1* plants was remarkably narrower, resulting in a wrinkled phenotype (Figure 9B,C). These results indicated that BrCWM is functional in *Arabidopsis*.

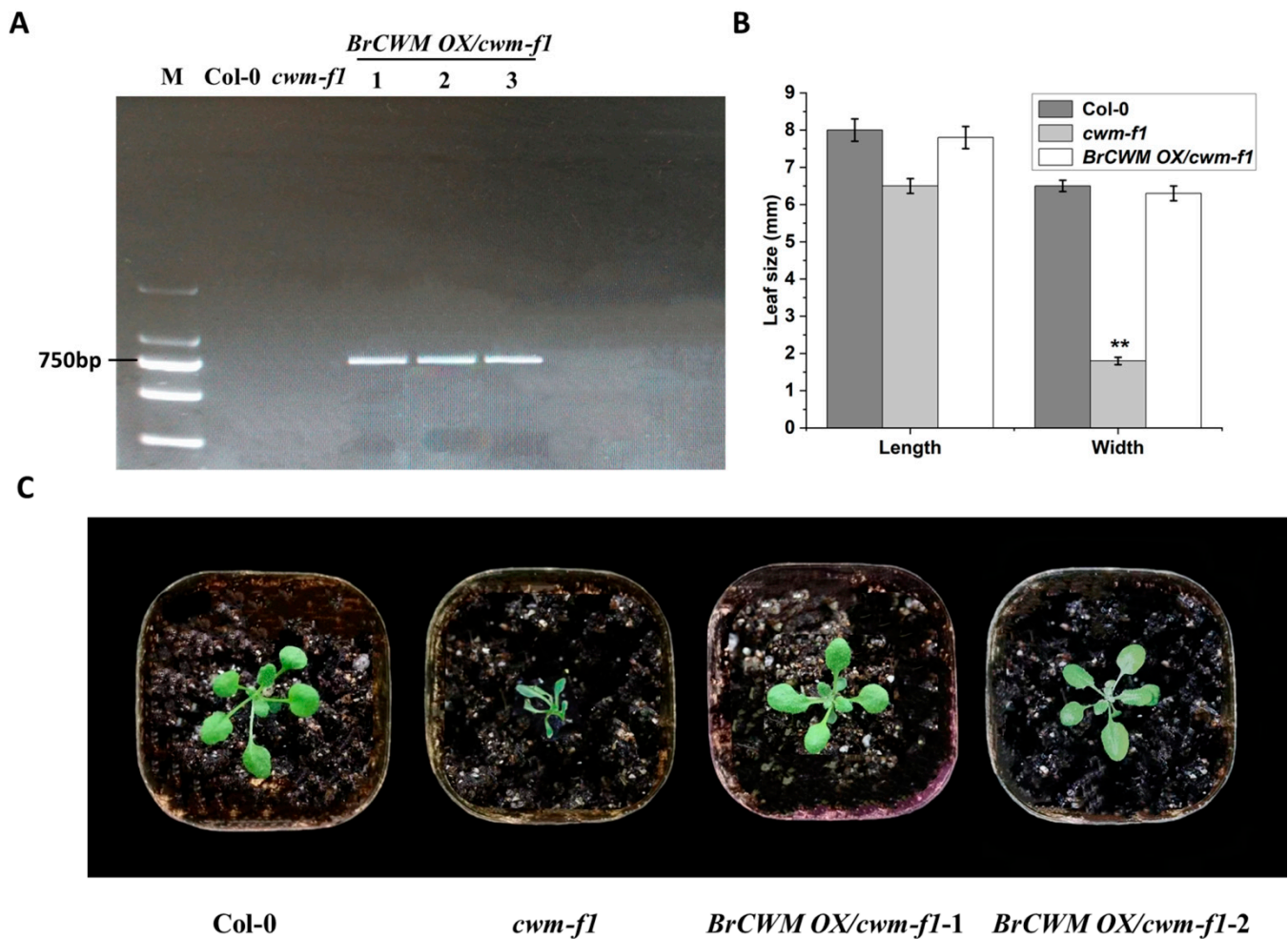


**Figure 9.** Transgenic functional verification of *BrCWM*. (A) Identification of the transgenic lines based on the PCR amplification of the cDNA sequence of *BrCWM* in *Arabidopsis*. M referred to molecular size markers; *BrCWM OX/cwm-f1* referred to transgenic *Arabidopsis* plants expressing *BrCWM*. (B) Statistical analysis of leaf length and width of Col-0, *cwm-f1*, and *BrCWM OX/cwm-f1*. Values are the means  $\pm$  SD ( $n = 15$  seedlings). Statistically significant differences were calculated using Student's *t*-tests (\*\*  $p < 0.01$ ). (C) Morphology of Col-0, *cwm-f1*, *BrCWM OX/cwm-f1-1*, and *BrCWM OX/cwm-f1-2* in a 2-week-old.

### 3. Discussion

In this research, the *cwm* mutant with wrinkled leaves was obtained with EMS mutagenesis from a DH line 'FT' in Chinese cabbage. A recessive nuclear gene, *Brcwm*, which governed the mutant phenotype, was fine-mapped using BSR-seq and whole-genome resequencing. An SNP transition (C to T) in exon 4 of *BrCWM* caused an amino acid change from Pro to Ser, which was responsible for the wrinkled leaves in the mutant. Transgenic *BrCWM* rescued the mutant phenotype with wrinkled leaves in *Arabidopsis cwm-f1*. In conclusion, as a novel target gene, *BrCWM* is essential for leaf-flattening. These findings provide new insights into the potential molecular mechanisms of leaf morphogenesis and plant development in Chinese cabbage.

Moderately wrinkled leaves and compact plants can increase planting density and reduce leaf transpiration, resulting in improved photosynthetic efficiency and increased yield [19]. Leaf initiation, outgrowth, expansion, maturation, and polarity can affect leaf flattening to a certain extent. *KNOX1*, *CLV*, and *PIN1* influence leaf initiation, thereby affecting leaf shape [20–22]. *YABBY*, *HD-ZIP III*, *KANADI*, and *AUXIN RESPONSE FACTOR (ARF)* gene families have an influence on leaf adaxial or abaxial polarity specification [23–26]. The *GRF* gene family acts as a regulator of cell proliferation and regulates the size and

shape of the leaves [27]. In addition, *WOX* and *YUCCA* gene families are essential for leaf development [28,29].

Leaf flattening can be influenced by the known genes associated with leaf morphology. For example, the mutation of *NRL1*, which encodes a cellulose synthase-like protein, results in semi-rolled leaves in rice [30]. *REL* encodes a protein with DUF630 and DUF632 domains that give rise to leaf rolling in rice [31]. The mutation of *BnaA03.IAA7* blocked auxin signaling, resulting in crinkle leaves and dwarfing plants [32]. Our research found that as the candidate gene of leaf wrinkled mutation, *BraA07g021970.3C* encodes a homolog of TON1, which is relevant to cortical microtubule (CMT) organization. Previous studies have shown that CMTs influence cellulose microfibril orientation, which in turn determines cell morphology [33]. Cell wall development is regulated by interactions between several endomembrane systems and CMTs [34]. TON1 has been shown to interact with *Arabidopsis* CENTRIN [16]. Moreover, TRM1 interacts with TON1 in *Arabidopsis* [35]. In *Arabidopsis* and tomato leaves, the process of leaf flattening depends on the arrangement of CMTs parallel to the adaxial–abaxial axis of the leaf in the direction of maximum stress [36]. Changes in cellulose content and cell walls can affect rice leaf flattening [37]. Here, we found more vascular bundles in *cwm* with the paraffin section observation (Figure 2). Therefore, we hypothesized that more vascular bundles result in a wrinkled phenotype. The downregulation of *BrCWM* expression in *cwm* leaves (Figure 6) might disrupt the CMT-mediated orientation of cellulose microfibrils and affect the formation of vascular bundles, which lead to more vascular bundles, ultimately leading to a wrinkled leaf phenotype.

Previous studies have indicated that the *TON1* deletion mutant changed the orientation of the symmetric divisions, resulting in a shorter root length than the normal plant, and the mutant plants were dwarf and malformed [15,16]. Our study demonstrated that the root length was remarkably shorter in the mutant *cwm*, and the expression of *BrCWM* was significantly lower in the roots of *cwm* during the growth period (Figures S4 and S5). Our results are consistent with those of previous studies. Plant roots can absorb water and inorganic salts, and there is a correlation between roots and leaves, which together determine the growth and development of plants [38]. Thus, we hypothesized that the dysfunction of *BrCWM* results in the irregular orientation of the symmetric divisions in the roots of *cwm*, further inhibiting root development and its ability to absorb nutrients and water. Consequently, the aerial part had fewer nutrients and water, leading to the wrinkled leaf phenotype in *cwm*.

Our study verified that the mutation of *BrCWM* led to wrinkled leaves. This is the first study to show that cortical microtubule-related proteins may be involved in leaf flattening in Chinese cabbage. These results provide an entirely new perspective for exploring the molecular mechanisms of leaf flattening in Chinese cabbage.

## 4. Materials and Methods

### 4.1. Plant Materials and Growth Conditions

A Chinese cabbage doubled haploid (DH) line ‘FT’ was designated as wild type. The *cwm* mutant was generated using 0.8% EMS mutagenesis. The ‘701’ was a DH line of Chinese cabbage with a distant genetic background from ‘FT’. They were grown in plastic greenhouses at the Shenyang Agricultural University, Shenyang, China, in 2018.

Wild-type *Arabidopsis* (Col-0) was preserved at the Shenyang Agricultural University. *cwm-f1* (CS2107348) was obtained from Arabidopsis Biological Resource Center (ABRC, Columbus, OH, USA). The plants were grown in a culture room with a cycle of 16 h light/8 h dark and 80% relative humidity at 22 °C.

### 4.2. Growth Determination

Five *cwm* and ‘FT’ plants with consistent growth were randomly selected for investigation. The leaf length, leaf width, and plant width were determined every 3 d for 24 d, starting from the appearance of the third true leaf. At the end of the heading stage, the

length, width, and weight of the leafy heads were measured. The average value of the data for each group was used for plotting.

#### 4.3. Cytological Observation

To identify whether the phenotype of a wrinkled leaf was influenced by the change in cell morphology, the mesophyll cells of *cwm* and 'FT' were observed with a paraffin section. Several 2 cm \* 1 cm slices were cut from the same parts of the sixth true leaf of *cwm* and 'FT', which were immediately fixed in FAA containing 50% ethanol, 5% glacial acetic, and 10% formalin for 24 h at 25 °C. Subsequently, dehydration was performed using gradient alcohol concentrations (50–100%). The samples were then permeated with xylene. The samples were embedded in paraffin. A microtome (LeicaRM2016, Wetzlar, Germany) was used to treat the paraffin sections, and an optical microscope (Nikon ECLIPSE 80i, Tokyo, Japan) was used to observe the stained samples.

#### 4.4. Genetic Analysis

The F<sub>1</sub>, F<sub>2</sub>, and BC<sub>1</sub> generations were created to verify the genetic characteristics of the wrinkled leaf phenotype. 'FT' and *cwm* were crossed to generate F<sub>1</sub>. F<sub>1</sub> plants were self-pollinated to generate the F<sub>2</sub> population. F<sub>1</sub> and the parent of *cwm* or 'FT' were crossed to produce BC<sub>1</sub> generations. The Chi-square ( $\chi^2$ ) test was conducted to analyze the segregation ratios of the BC<sub>1</sub> and F<sub>2</sub> populations.

#### 4.5. BSR-Sequencing Analysis

The F<sub>2</sub> segregating population for BSR-Seq and mapping was derived from the crossing of *cwm* and '701'. The leaves of 35 individuals with mutant and normal traits were sampled from the F<sub>2</sub> population and divided into two mixed pools. TRIzol Reagent (Invitrogen, Carlsbad, CA, USA) and an RNeasy Mini Kit (Qiagen, Beijing, China) were used to extract total RNA from each sample. Total RNA quality was determined using an Agilent bioanalyzer 2100 (Agilent Technologies, Palo Alto, CA, USA). Library construction was performed using a NEBNext Ultra RNA Library Prep Kit (Illumina, San Diego, CA, USA).

Transcriptome sequencing of the two pools was conducted using the Illumina HiSeq platform GENEWIZ (Suzhou, China). Cutadapt (version 1.9.1) was used to pretreat the raw reads, filter low-quality data, and eliminate pollution and connector sequences. The comparison results were compiled using Samtools (version 1.3.1) to obtain the possible single nucleotide variant (SNV) results that were annotated using Annovar software. According to the top 1% of the Euclidean distance<sup>5</sup> (ED<sup>5</sup>) value of the differential SNV and the distribution map of the differential SNV on chromosomes, chromosome segments related to the traits were located.

#### 4.6. DNA Extraction, Primer Design, and PCR

The genomic DNA of the leaves or roots was extracted using the cetyltrimethylammonium bromide (CTAB) method. The DNA concentration was regulated to approximately 30 ng/ $\mu$ L.

Initially, SSR markers were designed and polymorphic markers were screened using polyacrylamide gel electrophoresis between *cwm* and '701'. Other SSR markers and Indel markers were designed to narrow the mapping range using Primer Premier software (version 5.0) and synthesized in Sangon (Shanghai, China) (Table S1).

The PCR was conducted in a 10  $\mu$ L volume and started with a step of 95 °C for 5 min, followed by 35 cycles of 95 °C for 30 s and 56 °C for 30 s and with a final extension at 72 °C for 5 min.

#### 4.7. Whole-Genome Re-Sequencing

A library with 400bp inserted fragments was constructed and paired-end (PE) sequencing of the library was carried out using Next Generation Sequencing (NGS). High-quality data were obtained with the removal of joint contamination using Adapter Removal [39],

quality filtering, and length filtering. Using mapping between the reference genome (<http://brassicadb.cn/>, accessed on 5 May 2022) and high-quality data using BWA-MEM, single nucleotide polymorphism (SNP), insertion and deletion (INDEL), copy number variation (CNV), and structural variation of the chromosome (SV) were screened. GATK [40] and ANNOVAR [41] were used for SNP detection and annotation, respectively.

#### 4.8. Clone Sequencing

To verify the SNP mutation in *BrCWM*, the full-length sequence of *BrCWM* was obtained using cloning and sequencing. The cloning primer, C-1, was designed as shown in Table S2. The PCR products were linked using the Biorun Seamless Cloning Kit(#RDA01) (Biorun, Wuhan, China) and then transformed into competent cells (Biorun, Wuhan, China). The positive clones were sequenced using GENEWIZ (Tianjin, China), and the sequences were aligned using DNAMAN (version 5.2.9).

#### 4.9. Quantitative Reverse Transcriptase PCR (qRT-PCR)

To confirm the candidate gene expression pattern, a plant total RNA extraction kit (Tiangen, Beijing, China) was used to extract total RNA from roots and leaves at the fifth true leaf stage of 'FT' and *cwm* seedlings. The FastQuant RT Super Mix (Tiangen, Beijing, China) was used to synthesize cDNA. The primer RT-1 designed by Primer Premier 5.0 (Table S3) and the SYBR Green PCR Master Mix (Takara Bio Inc., Kusatsu, Japan) were used for qRT-PCR. The data were analyzed using QuantStudio™ Real-Time PCR software. The program and reaction volume of the qRT-PCR were described previously [42].

#### 4.10. Bioinformatic Analysis

TMHMM-2.0 (<https://www.cbs.dtu.dk/services/TMHMM-2.0/>, accessed on 5 May 2022) was used to predict the transmembrane domain of *BrCWM*. The protein tertiary structure of *BrCWM* was predicted using SWISS-MODEL software (<https://swissmodel.expasy.org/>, accessed on 5 May 2022). The phylogenetic tree of *BrCWM* was established using MEGA7.0.26 (<https://www.megasoftware.net>, accessed on 5 May 2022).

#### 4.11. Vector Construction and Arabidopsis Genetic Transformation

Homologous recombination and Golden Gate seamless cloning [43] were used for vector construction. The sequence of *BrCWM* was amplified from genomic DNA using the V-1 primer, as shown in Table S4, and recombined with pBWA(V)HS-ccdb-GFP. Then, 35S: *BrCWM*: GFP was introduced into *Arabidopsis* mutant *cwm-fl* with Agrobacterium-mediated genetic transformation. The inflorescences were dipped in bacterial solution for 2–3 s, then kept at humidity >90% using membrane sealing and incubated them in dark at 25 °C for 24 h. The impregnation cycle was seven days, with three times in total. The seeds were collected and sown. Positive transgenic plants were screened and raised to the 6–8th true leaf stage used for trait identification.

**Supplementary Materials:** The following supporting information can be downloaded at: <https://www.mdpi.com/article/10.3390/ijms24065225/s1>.

**Author Contributions:** H.F., C.W. and Y.W. designed the experiments. Y.W. conducted the experiments and wrote the manuscript. S.H. and Y.W. performed data analyses. Y.X. participated in laboratory experiments. H.F. and J.Z. revised the manuscript. All authors have read and agreed to the published version of the manuscript.

**Funding:** The research was supported by the National Natural Science Foundation of China (Grant No. 31972405).

**Data Availability Statement:** The raw sequence data of the BSR-Seq have been uploaded to the Sequence Read Archive at NCBI under the accession number SRR23004873 and SRR23004874. The raw sequence data of the whole genome re-sequencing have been uploaded to the Sequence Read Archive at NCBI under the accession number SRR23004840.

**Conflicts of Interest:** The authors declare that the research was conducted in the absence of any commercial or financial relationships that could be construed as a potential conflict of interest.

## References

- Huang, G.; Yang, Y.; Zhu, L.; Ren, X.; Peng, S.; Li, Y. The structural correlations and the physiological functions of stomatal morphology and leaf structures in C3 annual crops. *Planta* **2022**, *256*, 39. [\[CrossRef\]](#)
- Liu, Q.; Huang, Z.; Wang, Z.; Chen, Y.; Wen, Z.; Liu, B.; Tigabu, M. Responses of leaf morphology, NSCs contents and C:N:P stoichiometry of *Cunninghamia lanceolata* and *Schima superba* to shading. *BMC Plant Biol.* **2020**, *20*, 354. [\[CrossRef\]](#) [\[PubMed\]](#)
- Lee, S.-M.; Song, H.; Yi, H.; Hur, Y. Transcriptomic analysis of contrasting inbred lines and F2 segregant of Chinese cabbage provides valuable information on leaf morphology. *Genes Genom.* **2019**, *41*, 811–829. [\[CrossRef\]](#) [\[PubMed\]](#)
- Huang, C.; Yang, M.; Shao, D.; Wang, Y.; Wan, S.; He, J.; Meng, Z.; Guan, R. Fine mapping of the BnUC2 locus related to leaf up-curling and plant semi-dwarfing in *Brassica napus*. *BMC Genom.* **2020**, *21*, 530. [\[CrossRef\]](#)
- Rong, F.; Chen, F.; Huang, L.; Zhang, J.; Zhang, C.; Hou, D.; Cheng, Z.; Weng, Y.; Chen, P.; Li, Y. A mutation in class III homeodomain-leucine zipper (HD-ZIP III) transcription factor results in curly leaf (cul) in cucumber (*Cucumis sativus* L.). *Theor. Appl. Genet.* **2019**, *132*, 113–123. [\[CrossRef\]](#) [\[PubMed\]](#)
- Gong, X.; Wang, F.; Chen, H.; Liu, X.; Zhang, S.; Zhao, J.; Yi, J. Genetic Mapping and Transcriptomic Analysis Revealed the Molecular Mechanism Underlying Leaf-Rolling and a Candidate Protein Phosphatase Gene for the Rolled Leaf-Dominant (RL-D) Mutant in Rice. *Plant Mol. Biol. Report.* **2022**, *40*, 256–270. [\[CrossRef\]](#)
- Adedze, Y.M.N.; Feng, B.; Shi, L.; Sheng, Z.; Tang, S.; Wei, X.; Hu, P. Further insight into the role of KAN1, a member of KANADI transcription factor family in rice. *Plant Growth Regul.* **2018**, *84*, 237–248. [\[CrossRef\]](#)
- de Keijzer, J.; Mulder, B.M.; Janson, M.E. Microtubule networks for plant cell division. *Syst. Synth. Biol.* **2014**, *8*, 187–194. [\[CrossRef\]](#)
- Jain, K.; Yadav, S.A.; Athale, C.A. Number Dependence of Microtubule Collective Transport by Kinesin and Dynein. *J. Indian Inst. Sci.* **2021**, *101*, 19–30. [\[CrossRef\]](#)
- Schwarzerová, K.; García-González, J. Cortical Region of Diffusively Growing Cells as a Site of Actin–Microtubule Cooperation in Cell Wall Synthesis. In *The Cytoskeleton: Diverse Roles in a Plant's Life*; Sahi, V.P., Baluška, F., Eds.; Springer International Publishing: Cham, Switzerland, 2019; pp. 1–21.
- Dhonukshe, P.; Mathur, J.; Hülskamp, M.; Gadella, T.W.J. Microtubule plus-ends reveal essential links between intracellular polarization and localized modulation of endocytosis during division-plane establishment in plant cells. *BMC Biol.* **2005**, *3*, 11. [\[CrossRef\]](#)
- Hush, J.M.; Overall, R.L. Re-orientation of cortical F-actin is not necessary for wound-induced microtubule re-orientation and cell polarity establishment. *Protoplasma* **1992**, *169*, 97–106. [\[CrossRef\]](#)
- Zhang, L.; Ambrose, C. CLASP balances two competing cell division plane cues during leaf development. *Nat. Plants* **2022**, *8*, 682–693. [\[CrossRef\]](#) [\[PubMed\]](#)
- Müller, S.; Han, S.; Smith, L.G. Two Kinesins Are Involved in the Spatial Control of Cytokinesis in *Arabidopsis thaliana*. *Curr. Biol.* **2006**, *16*, 888–894. [\[CrossRef\]](#)
- Zhang, Y.; Iakovidis, M.; Costa, S. Control of patterns of symmetric cell division in the epidermal and cortical tissues of the *Arabidopsis* root. *Development* **2016**, *143*, 978–982. [\[CrossRef\]](#) [\[PubMed\]](#)
- Spinner, L.; Pastuglia, M.; Belcram, K.; Pegoraro, M.; Goussot, M.; Bouchez, D.; Schaefer, D.G. The function of TONNEAU1 in moss reveals ancient mechanisms of division plane specification and cell elongation in land plants. *Development* **2010**, *137*, 2733–2742. [\[CrossRef\]](#)
- Whittington, A.T.; Vugrek, O.; Wei, K.J.; Hasenbein, N.G.; Sugimoto, K.; Rashbrooke, M.C.; Wasteneys, G.O. MOR1 is essential for organizing cortical microtubules in plants. *Nature* **2001**, *411*, 610–613. [\[CrossRef\]](#) [\[PubMed\]](#)
- Azimzadeh, J.; Nacry, P.; Christodoulidou, A.; Drevensek, S.P.; Camilleri, C.; Amiour, N.; Parcy, F.O.; Pastuglia, M.; Bouchez, D. *Arabidopsis* TONNEAU1 Proteins Are Essential for Preprophase Band Formation and Interact with Centrin. *Plant Cell* **2008**, *20*, 2146–2159. [\[CrossRef\]](#)
- Sarieva, G.E.; Kenzhebaeva, S.S.; Lichtenthaler, H.K. Adaptation potential of photosynthesis in wheat cultivars with a capability of leaf rolling under high temperature conditions. *Russ. J. Plant Physiol.* **2010**, *57*, 28–36. [\[CrossRef\]](#)
- Chang, L.; Mei, G.; Hu, Y.; Deng, J.; Zhang, T. LMI1-like and KNOX1 genes coordinately regulate plant leaf development in dicotyledons. *Plant Mol. Biol.* **2019**, *99*, 449–460. [\[CrossRef\]](#)
- Nidhi, S.; Preciado, J.; Tie, L. Knox homologs shoot meristemless (STM) and KNAT6 are epistatic to CLAVATA3 (CLV3) during shoot meristem development in *Arabidopsis thaliana*. *Mol. Biol. Rep.* **2021**, *48*, 6291–6302. [\[CrossRef\]](#)
- Qu, C.; Bian, X.; Han, R.; Jiang, J.; Yu, Q.; Liu, G. Expression of BpPIN is associated with IAA levels and the formation of lobed leaves in *Betula pendula* ‘Dalecartica’. *J. For. Res.* **2020**, *31*, 87–97. [\[CrossRef\]](#)
- Li, Y.-Y.; Shen, A.; Xiong, W.; Sun, Q.-L.; Luo, Q.; Song, T.; Li, Z.-L.; Luan, W.-J. Overexpression of OsHox32 Results in Pleiotropic Effects on Plant Type Architecture and Leaf Development in Rice. *Rice* **2016**, *9*, 46. [\[CrossRef\]](#) [\[PubMed\]](#)
- Kerstetter, R.A.; Bollman, K.; Taylor, R.A.; Bomblies, K.; Poethig, R.S. KANADI regulates organ polarity in *Arabidopsis*. *Nature* **2001**, *411*, 706–709. [\[CrossRef\]](#) [\[PubMed\]](#)

25. Burian, A.; Paszkiewicz, G.; Nguyen, K.T.; Meda, S.; Raczynska-Szajgin, M.; Timmermans, M.C.P. Specification of leaf dorsiventrality via a prepatterned binary readout of a uniform auxin input. *Nat. Plants* **2022**, *8*, 269–280. [[CrossRef](#)]
26. Zhang, T.; Li, C.; Li, D.; Liu, Y.; Yang, X. Roles of YABBY transcription factors in the modulation of morphogenesis, development, and phytohormone and stress responses in plants. *J. Plant Res.* **2020**, *133*, 751–763. [[CrossRef](#)] [[PubMed](#)]
27. Lu, Y.; Meng, Y.; Zeng, J.; Luo, Y.; Feng, Z.; Bian, L.; Gao, S. Coordination between GROWTH-REGULATING FACTOR1 and GRF-INTERACTING FACTOR1 plays a key role in regulating leaf growth in rice. *BMC Plant Biol.* **2020**, *20*, 200. [[CrossRef](#)]
28. Tvorogova, V.E.; Krasnoperova, E.Y.; Potsenkovskaia, E.A.; Kudriashov, A.A.; Dodueva, I.E.; Lutova, L.A. What Does the WOX Say? Review of Regulators, Targets, Partners. *Mol. Biol.* **2021**, *55*, 311–337. [[CrossRef](#)]
29. Woo, Y.-M.; Park, H.-J.; Su'udi, M.; Yang, J.-I.; Park, J.-J.; Back, K.; Park, Y.-M.; An, G. Constitutively wilted 1, a member of the rice YUCCA gene family, is required for maintaining water homeostasis and an appropriate root to shoot ratio. *Plant Mol. Biol.* **2007**, *65*, 125–136. [[CrossRef](#)]
30. Hu, J.; Zhu, L.; Zeng, D.; Gao, Z.; Guo, L.; Fang, Y.; Zhang, G.; Dong, G.; Yan, M.; Liu, J.; et al. Identification and characterization of NARROW ANDROLLED LEAF 1, a novel gene regulating leaf morphology and plant architecture in rice. *Plant Mol. Biol.* **2010**, *73*, 283–292. [[CrossRef](#)]
31. Yang, S.-Q.; Li, W.-Q.; Miao, H.; Gan, P.-F.; Qiao, L.; Chang, Y.-L.; Shi, C.-H.; Chen, K.-M. REL2, A Gene Encoding An Unknown Function Protein which Contains DUF630 and DUF632 Domains Controls Leaf Rolling in Rice. *Rice* **2016**, *9*, 37. [[CrossRef](#)]
32. Ping, X.; Ye, Q.; Yan, M.; Zeng, J.; Yan, X.; Li, H.; Li, J.; Liu, L. Integrated genetic mapping and transcriptome analysis reveal the BnaA03. IAA7 protein regulates plant architecture and gibberellin signaling in *Brassica napus* L. *Theor. Appl. Genet.* **2022**, *135*, 3497–3510. [[CrossRef](#)] [[PubMed](#)]
33. Baskin, T.I. On the alignment of cellulose microfibrils by cortical microtubules: A review and a model. *Protoplasma* **2001**, *215*, 150–171. [[CrossRef](#)] [[PubMed](#)]
34. Oda, Y. Emerging roles of cortical microtubule–membrane interactions. *J. Plant Res.* **2018**, *131*, 5–14. [[CrossRef](#)]
35. Drevensek, S.; Goussot, M.; Duroc, Y.; Christodoulidou, A.; Steyaert, S.; Schaefer, E.; Duvernois, E.; Grandjean, O.; Vantard, M.; Bouchez, D.; et al. The Arabidopsis TRM1–TON1 Interaction Reveals a Recruitment Network Common to Plant Cortical Microtubule Arrays and Eukaryotic Centrosomes. *Plant Cell* **2012**, *24*, 178–191. [[CrossRef](#)] [[PubMed](#)]
36. Zhao, F.; Du, F.; Oliveri, H.; Zhou, L.; Ali, O.; Chen, W.; Feng, S.; Wang, Q.; Lü, S.; Long, M.; et al. Microtubule-Mediated Wall Anisotropy Contributes to Leaf Blade Flattening. *Curr. Biol.* **2020**, *30*, 3972–3985. [[CrossRef](#)] [[PubMed](#)]
37. Alamin, M.; Zeng, D.-D.; Sultana, M.H.; Qin, R.; Jin, X.-L.; Shi, C.-H. Photosynthesis, cellulose contents and ultrastructure changes of mutant rice leading to screw flag leaf. *Plant Growth Regul.* **2018**, *85*, 1–13. [[CrossRef](#)]
38. Navarro, J.M.; Garrido, C.; Martínez, V.; Carvajal, M. Water relations and xylem transport of nutrients in pepper plants grown under two different salts stress regimes. *Plant Growth Regul.* **2003**, *41*, 237–245. [[CrossRef](#)]
39. Schubert, M.; Lindgreen, S.; Orlando, L. AdapterRemoval v2: Rapid adapter trimming, identification, and read merging. *BMC Res. Notes* **2016**, *9*, 88. [[CrossRef](#)]
40. Zhu, P.; He, L.; Li, Y.; Huang, W.; Xi, F.; Lin, L.; Zhi, Q.; Zhang, W.; Tang, Y.T.; Geng, C.; et al. OTG-snp caller: An optimized pipeline based on TMAP and GATK for SNP calling from ion torrent data. *PLoS ONE* **2014**, *9*, e97507. [[CrossRef](#)]
41. Wang, K.; Li, M.; Hakonarson, H. ANNOVAR: Functional annotation of genetic variants from high-throughput sequencing data. *Nucleic Acids Res.* **2010**, *38*, e164. [[CrossRef](#)]
42. Zhao, Y.; Huang, S.; Zhang, M.; Zhang, Y.; Feng, H. Mapping of a Pale Green Mutant Gene and Its Functional Verification by Allelic Mutations in Chinese Cabbage (*Brassica rapa* L. ssp. *pekinensis*). *Front. Plant Sci.* **2021**, *12*, 699308. [[CrossRef](#)] [[PubMed](#)]
43. Engler, C.; Kandzia, R.; Marillonnet, S. A one pot, one step, precision cloning method with high throughput capability. *PLoS ONE* **2008**, *3*, e3647. [[CrossRef](#)] [[PubMed](#)]

**Disclaimer/Publisher's Note:** The statements, opinions and data contained in all publications are solely those of the individual author(s) and contributor(s) and not of MDPI and/or the editor(s). MDPI and/or the editor(s) disclaim responsibility for any injury to people or property resulting from any ideas, methods, instructions or products referred to in the content.